

Computationally Identified Novel Diphenyl- and Phenylpyridine Androgen Receptor Antagonist Structures

Annu A. Söderholm,^{†,‡} Johanna Viiliäinen,[§] Pekka T. Lehtovuori,[†] Hanna Eskelinen,[§]
Daniela Roell,^{||} Aria Baniahmad,^{§,||} and Tommi H. Nyrönen^{*,†}

CSC—Scientific Computing Ltd., PO Box 405, FI-02101 Espoo, Finland, Department of Biochemistry and Pharmacy, Åbo Akademi University, PO Box 66, FI-20521 Turku, Finland, Department of Biochemistry, University of Kuopio, PO Box 1627, FI-70211 Kuopio, Finland, Institute of Human Genetics and Anthropology, Friedrich Schiller University, 07740 Jena, Germany

Received April 30, 2008

We have identified and profiled a set of androgen receptor (AR) binding compounds representing two nonsteroidal scaffolds from a public chemical database supplied by Asinex with virtual screening procedure incorporating our recently published 3D QSAR model of AR ligands. The diphenyl- and phenylpyridine-based compounds act as antagonists in wild-type AR in CV1 cells and also retain this antagonistic character in CV1 cells expressing T877A mutant receptor. This mutation is frequently associated with prostate cancer. Two of the compounds repress the androgen-dependent cell growth of LNCaP prostate cancer cells expressing the T877A AR mutant. Molecular modeling of the observed in vitro antagonism with induced fit docking suggests that W741 and M895 could be mechanistically involved in the initiation of the antagonism. The results indicate finding of nonsteroidal AR antagonist compounds from a public chemical database with computational methods. Compounds could serve as a novel platform to develop more potent AR antagonists with inhibitory activity in both wild-type and T877A mutant AR.

INTRODUCTION

Even if steroids are the natural ligands for androgen receptor (AR), the trend within the nuclear receptor (NR) field is to develop drugs with nonsteroidal structures. It is thought that the nonsteroids enable improved receptor specificity and reduced side-effect profiles, in addition to being easier to modify compared to steroids. At present, only three nonsteroidal AR-targeted antiandrogens (flutamide, nilutamide, and bicalutamide) are on the market, but effort has been put into finding new nonsteroidal antiandrogen leads for drug discovery programs.^{1,2} Antiandrogens are needed particularly for treatment of prostate cancer (CaP), which is the most common cancer in men in Western countries. CaP is often accompanied with AR gene mutations,³ which render the receptor susceptible to activation by a broadened spectrum of ligands including antiandrogens. Therefore, design of antiandrogens that retain their inhibitory activity in mutated AR variants, in addition to the wild-type AR, is of importance.

By itself, AR is considered transcriptionally inactive. Signaling is initiated by the binding ligands. Activation of AR pathways requires binding of a natural or synthetic androgen (agonist) to the ligand binding pocket (LBP) of the C-terminal ligand binding domain (LBD) of the AR structure. In response to androgen binding, the LBD structure rearranges in such a way that a hydrophobic cleft (activation

function 2 or AF2), which is important for AR activation, is presented on the surface of the LBD. The structural basis for inhibition of the AR signaling pathways by design antiandrogen (antagonist) binding to the AR LBP is not resolved, but various ideas have been suggested.^{4–8} Together, over fifty crystallographically determined structures of AR ligand binding domain (LBD) are reported in the protein data bank (PDB)⁹ (<http://www.rcsb.org/pdb>) at the time of writing. These structures provide good basis for a knowledge-based structural search for new AR ligands.

In an effort to find new nonsteroidal scaffolds as AR ligands, we performed receptor-based virtual screening (VS) of a public chemical database. The VS protocol integrates our 3D QSAR model of AR ligands¹⁰ for prioritizing the docked database compounds for experimental binding affinity (IC₅₀) determination for AR. The 3D QSAR model was built from AR ligands with various activity profiles, and as such, it is able to predict binding affinities for potential AR ligands without consideration to their possible modulation of AR's ligand-gated transcription. The resulting model is statistically significant, and its interpretation is consistent with the structural features of the AR LBP. Importantly, it can be integrated in VS because it uses AR ligands aligned with automated docking. In general, 3D QSAR methods based on an overlay of molecules (such as CoMFA¹¹ and CoMSIA¹²) are not often integrated in VS because of the prevailing opinion that such models lack credibility to identify novel active molecules for a specific target by VS. Our experience proves otherwise.

Here, we report structures, binding (IC₅₀), and in vitro functional profiling of six new diphenyl- and phenylpyridine-based AR-binding compounds found with VS (Figure 1).

*To whom correspondence should be addressed. Phone: +358-9-4572235. Fax: +358-9-4572302. E-mail: tommi.nyronen@csc.fi.

[†] CSC—Scientific Computing Ltd.

[‡] Åbo Akademi University.

[§] University of Kuopio.

^{||} Friedrich Schiller University.

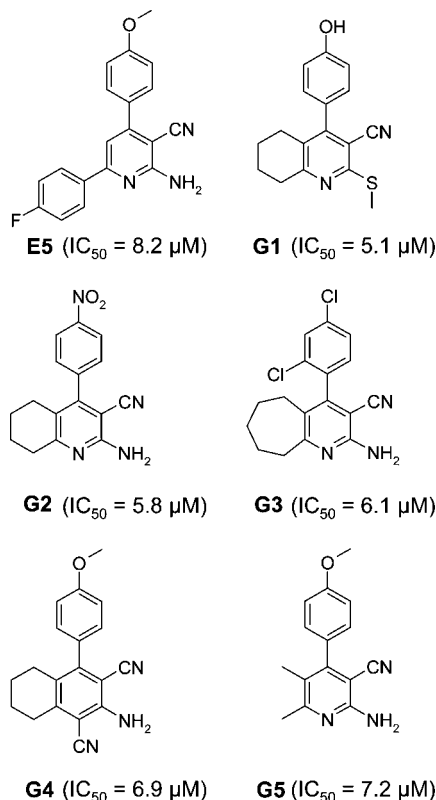


Figure 1. Chemical structures of the compounds ordered from Asinex (<http://www.asinex.com>) for investigation of their AR binding and functional activity. The IC_{50} values (μ M) for replacement of Fluormone for the wild-type AR are shown in the parentheses.

Activity profiling of reported compounds was performed using reporter gene assays (CV1 cell line) and prostate cancer cell growth assays (LNCaP cell line). The assays provide knowledge of the biological effects that the compounds induce when they interact with wild-type (CV1) or mutant (CV1 and LNCaP) AR LBD structures. Agonism was not observed for any of the compounds. Rather, a range of antagonistic effects was displayed by the compounds in the reporter assays with either wild-type or mutant AR LBD. Suppression of prostate cancer cell growth was detected for two compounds. The results suggest a discovery of two nonsteroidal antagonist structures with inhibitory activity in both wild-type and mutant AR LBD structures with computational methods. Results from induced fit docking simulations suggest binding modes for these small-sized micromolar ligands and allow discussion of possible ligand-induced changes in receptor structure that lead to antagonism.

METHODS

VS-Based Compound Selection. The computational search for AR ligands was carried out on a commercial compound library provided by Asinex (<http://www.asinex.com>). The Asinex Gold Collection comprising 219 680 compounds (2005/03) was used as the screening database in the VS. In our receptor-based VS protocol docking was combined with binding affinity prediction using our previously generated 3D QSAR model of AR ligands.¹⁰ Docking was carried out with program GOLD.¹³ For each docked compound, ten possible poses were first produced using the docking procedure reported in Söderholm et al.¹⁰ Our 3D

QSAR model was used to predict the affinity for each of these poses, and the one that was predicted to be the best was picked as the representative pose for the molecule under consideration. The binding affinities for these poses provided the basis for rank-ordering of the database compounds. Top-ranked compounds were visually checked to ensure that the docked conformations and the interactions with the protein make sense. This procedure removes possible false 3D QSAR predictions in cases where the predicted molecule is not docked to the model's coverage area. Selection of compounds for experimental binding affinity determination (IC_{50}) was finally based on a few potential top-ranked compound scaffolds, which were expanded into a small series of closely related compounds. Compounds were ordered as DMSO solution from Asinex Europe and have a minimum purity of 90%.

The structures of six diphenyl- and phenylpyridine-based compounds (Figure 1), which were selected for experimental testing with the above-described protocol, represent compounds from two structurally distinct scaffolds called E and G (internal compound nomenclature). The chemical structures of E compounds differ from the G compounds when their similarity is evaluated with computational methods, like the Tanimoto similarity scores. The E compounds have two substituted phenyls linked to substituted pyridine, whereas G compounds have a single substituted phenyl attached to a substituted pyridine. These compounds differ from compounds used to train the model¹⁰ and have not, to our best knowledge, been reported before as AR ligands.

Receptor Binding Assay. Fluorescence polarization assays were performed to analyze the *in vitro* binding of nonsteroidal compounds to AR. Rat AR LBD protein, which is identical to the human AR LBD, was added to a fluorescent androgen ligand (Fluormone AL Green, Invitrogen, Carlsbad, CA) to form an AL Green/AR complex with high fluorescence polarization. The complex was added to eight different concentrations (from 1×10^{-8} to 3×10^{-5} M) of test compound in 384-well microplate. The concentration of the test compound that results in a half-maximal shift in polarization value equals the IC_{50} of the test compound, which is a measure of the relative affinity of the test compound for the receptor LBD. The IC_{50} values were determined from single dilution series measurements. The experiments were performed using Androgen Receptor Competitor Assay Kit and according to the instructions of the manufacturer (Invitrogen). The polarization values were measured from the microplate by Ultra microplate fluorometer (Tecan, Switzerland), and results were calculated with Prism software (GraphPad).

Cotransfection Assay. Monkey kidney CV1 cells were chosen because they lack endogenous functional androgen, progesterone, and glucocorticoid receptors that might interfere with the assay system because these related receptors bind to the same reporter. Cells were seeded onto 6-well tissue culture plates at 1.2×10^5 cells per well and grown in DMEM medium supplemented with 10% charcoal-stripped fetal bovine serum (FBS). Six hours later cells were transfected using $Ca_3(PO_4)_2$ method.¹⁴ The hAR or AR T877A expression vector, pSG5-hAR (0.2 μ g), was cotransfected with 1 μ g of the reporter plasmid pMMTV-luc and 0.2 μ g of the pCMV-LacZ expression vector for the β -galactosidase as internal control for transfection efficiency. After 12 h, media were replaced either with or without the

addition of 3×10^{-10} M R1881 (methyltrienolone, Perkin-Elmer), together with the indicated compound at 10 μ M final concentration. After 48 h, cells were harvested and assayed for both luciferase and β -galactosidase activity. Each value obtained with luciferase assay was normalized to that obtained with β -galactosidase activity from the same cellular extract. All transfection assays shown were performed in triplicate and were repeated at least three times. Cell morphology was detected with light microscope.

Cell Growth Assay. LNCaP cells¹⁵ were seeded onto 24-well tissue culture plates at 5×10^3 cells per well and grown in RPMI 1640 medium supplemented with 5% untreated FBS known to contain androgens. Cells were allowed to attach and grow for 72 h. At the indicated days, cells were harvested by trypsinization and counted by using a Bürker cell counting chamber. Media was replaced three times a week with addition of indicated compound at 10 μ M final concentration. All growth curve assays shown were performed in triplicate and were repeated at least twice.

Structure Preparation. Coordinates for the wild-type AR LBD structure (1i37)¹⁶ were obtained from the PDB.⁹ The structure was prepared with the Maestro software package of Schrödinger.¹⁷ Hydrogens were added to the structure, and the hydrogen bonds were optimized. Bond orders and formal charges were adjusted. All water molecules, except the structural water molecule between Q711 and R752, were removed. The missing side-chain atoms of residues 692 and 845–850 were predicted using Prime (version 1.6).¹⁸ To generate the AR LBD structure corresponding to that of the LNCaP cell line, the T877A mutation was introduced. The protein preparation was completed with a restrained minimization of both the wild-type and mutant receptor structures using an rmsd of 0.18 Å as a termination criterion.

The 3D coordinates for the ligands were generated with the program Corina (version 3.0).^{19,20} The correct bond orders and formal charges were assigned in Maestro. Minimization using the Impact program (version 4.5)²¹ with the OPLS 2005 force field was performed to conclude the ligand preparation.

Induced Fit Docking. The docking program GOLD,¹³ which considers ligand flexibility but ignores protein flexibility apart from optimization of –OH and –NH₃ group orientations, was used to initially dock compounds during the VS phase. To better understand the structural interactions between the protein and tested compounds, which appeared to have an antagonistic profile, we wanted to explore the induced conformational changes in the wild-type and T877A mutant AR structure. To gain insight into the changes induced to the receptor structure by the newly identified antagonists, induced fit docking protocol of Schrödinger,²² which has been described in detail elsewhere,²³ was used for ligand docking. The protocol uses the program Glide (version 4.5) for flexible ligand docking and the Refinement module of Prime (version 1.6) for prediction of structural changes on the receptor induced by the ligand.

The binding site for docking was defined using the center of the bound ligand (DHT) in the AR LBD structure, and the size was computed automatically from the size of the ligand. In the initial Glide docking, a maximum of 20 poses per ligand were generated using the softened-potential docking to reduce steric clashes (with van der Waals scaling factors of 0.5 for both receptor and ligand atoms). Prime

was subsequently used to predict the side chain conformations of residues within 5 Å of every ligand pose. Minimization of these residues, together with the ligand, gave an induced fit receptor structure for each of the initial docking poses. For every ligand, the induced fit receptor structures within 30 kcal/mol of the lowest-energy complex structure were then used as target binding sites in a second round of Glide docking, now with default Glide settings. Both docking steps were performed using the “standard precision” mode of Glide. The output docking poses were ranked according to IFDScore, which is a composite score of the docking score (GlideScore) and complex energy (Prime energy). All the final docking poses were visually inspected.

RESULTS

This article reports results from our in vitro functional profiling performed on a limited set of AR-binding compounds found with our VS protocol that integrates a previously published 3D QSAR¹⁰ and structural explanation for the observed ligand functionalities using advanced computational docking methods. The discovered compounds differ from ones used to train the 3D QSAR model and have not to the best of our knowledge been reported before as AR ligands. This case study thus illustrates the potentiality of alignment dependent 3D QSAR methods in combination with other computational methods as part of the hit/lead discovery process for specified target proteins.

Receptor Binding. The compounds (Figure 1) were all able to replace the high-affinity fluorescent ligand from the AR binding site (Fluormone AL Green, Invitrogen, Carlsbad, CA). The binding of the fluorescent ligand was reduced to half (IC₅₀) at 5–8 μ M concentrations. Because the affinity of the compounds was only at the micromolar range, further functional profiling had to be carried out at the 10 μ M concentration. Despite the high concentration, cells tolerated the compounds well.

The competition binding assay verified that the compounds interact with the AR LBD as predicted by computations. Binding affinity predictions from the 3D QSAR model do not correlate with the actual experimentally measured affinities however. In general, the inability to accurately predict binding affinities for docked compounds is a recognized weakness of all generally used scoring functions.^{24–26}

Inhibition of Transactivation of Wild-Type AR. The activity of the compounds E5, G1–G5 at 10 μ M concentration on transactivation of wild-type AR was analyzed in a reporter gene assay using the stable synthetic hormone methyltrienolone (R1881) (3×10^{-10} M) as a reference androgen to ensure stable assay conditions. The reporter gene assay was performed using CV1 cells, which were transiently cotransfected with the human AR and the MMTV-luc reporter gene, that is, the AR-responsive promoter.²⁷ To monitor the transfection efficiency, the CV1 cells were additionally cotransfected with the β -galactosidase gene as control. The CV1 cells were chosen for the reporter assays because they are devoid of endogenously expressed functional steroid receptors.²⁷ Thus, transfection with the AR-allowed receptor-specific responses to be measured. Because the transfected AR was in the natural form, the effects on AR transactivation measure the compound activity toward the wild-type receptor.

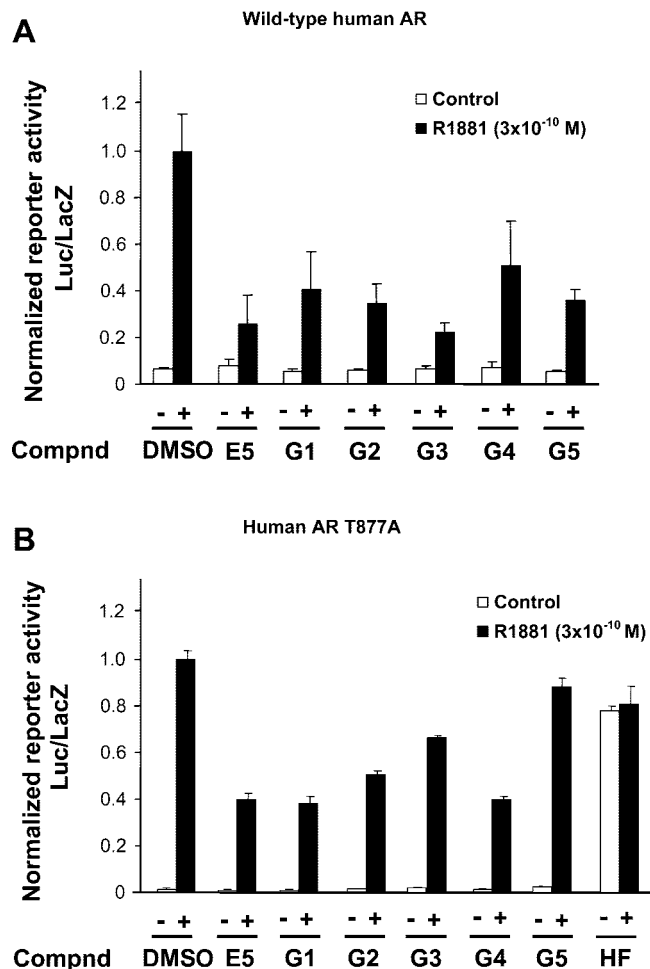


Figure 2. Nonsteroidal AR binding compounds repress AR-mediated transactivation. CV1 cells were transfected with the wild-type human AR expression vector (A) or the mutant AR T877A expression vector (B), MMTV-luc reporter plasmid, and pCMV-LacZ expression vector for internal normalization. Cells were treated 48 h with (black bars) or without (white bars) 10^{-10} M methyltrienolone (R1881), together with the indicated compound at 10 μ M final concentration. HF was used at 0.1 μ M concentration. Control is solvent alone. Control values in the absence of ligand are set arbitrarily as one. (A) Assays using the wild-type human AR. (B) Assays using the AR T877A mutant.

To study whether the tested compounds have intrinsic agonist activity, the reporter assay was also performed in the absence of R1881. None of the compounds increased the luciferase reporter activity at a concentration of 10 μ M compared to the DMSO control, indicating lack of agonist activity. On the contrary, the reporter assay demonstrated that at 10 μ M these compounds exhibited noticeable antagonist activity by inhibiting the R1881 induced transactivation of AR. The most potent antagonism was observed for compounds G3 and E5, followed by compounds G2 and G5 and finally by G1 and G4 (Figure 2A).

Effects on Proliferation of LNCaP Cells. The LNCaP cells are used as a model cell line for CaP. These cells are known to grow in an androgen-dependent manner. Interestingly, they express AR with a binding site mutation (T877A), often found in CaP patients.²⁸ This mutation converts the pure antagonist hydroxyflutamide (HF) for the wild-type AR into an agonist for the mutant AR.^{29,30}

Before performing LNCaP experiments, the compounds were first analyzed for transactivation of the AR T877A

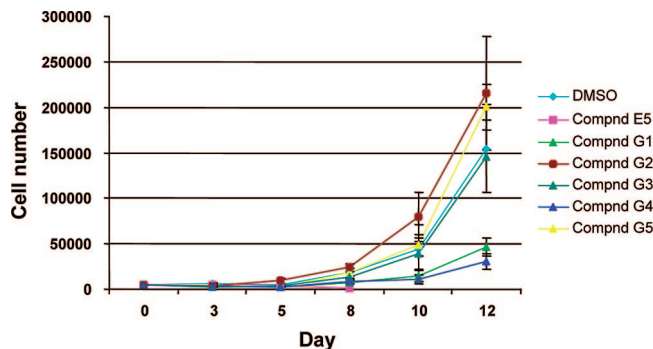


Figure 3. Nonsteroidal AR binding compounds influence LNCaP prostate cancer cell growth. LNCaP cells were used for cell growth assays. LNCaP cells were seeded onto 24-well tissue culture plates at 5000 cells per well and grown in RPMI 1640 medium supplemented with 5% normal, untreated FBS containing endogenous androgens. Cells were incubated with the indicated compounds at 10 μ M final concentration and counted at the indicated days. Control cells were treated with the solvent DMSO.

mutant receptor using a similar experimental setup as with wild-type CV1 cells but with an expression vector for the human AR T877A mutant (Figure 2B). Compounds E5, G1, and G4 are effective antagonists in the CV1 cells expressing the mutant receptor. Compound G2 also clearly inhibits transactivation in cell line with mutant AR but to a lesser extent than E5, G1, and G4. As can be observed, compounds G3 and G5 have only a marginal or no antagonism. Taken together, this suggests that the compounds act differently on the mutant AR T877A compared to wild-type AR. A similar change in behavior between mutant and wild-type AR also takes place in the case of the known AR antagonist HF.^{29,30} Notably, in contrast to HF, none of the compounds exert an agonistic activity for the mutant AR T877A. This finding corroborates that the discovered ligands affect AR transactivation through binding to the steroid binding pocket: their activity is significantly affected when a mutation is introduced within the binding pocket. The findings also suggest that these new nonsteroidal compounds exhibit a different underlying mechanism for AR antagonism as compared to HF.

Thereafter, the effects of the identified AR antagonists on the proliferation of LNCaP cells were examined. The response of LNCaP cell growth to the antagonist treatment was studied at a concentration of 10 μ M in culture medium supplemented with 5% normal serum, which contains natural androgens to sustain normal cell growth. The proliferation of LNCaP cells treated with DMSO as the vehicle served as control.

Three kinds of proliferative response were observed in LNCaP cells (Figure 3). First, a significant repression of cell growth was observed from the very first days of treatment with compounds G1 and G4. This observation is in line with the antagonist character of G1 and G4 on AR transactivation in mutant CV1 cells. The level of suppression of LNCaP proliferation was substantially the same for both of these two antagonists. Second, the growth rate of LNCaP cells following treatment with compounds G2, G3, or G5 did not exhibit statistically significant difference to the growth rate observed for DMSO-treated control cells, even if the proliferative effect of compounds G2 and G5 is seemingly stimulatory. Although G2 inhibited the AR T877A mediated transactivation in CV1 cells, G5 only inactivated the wild-

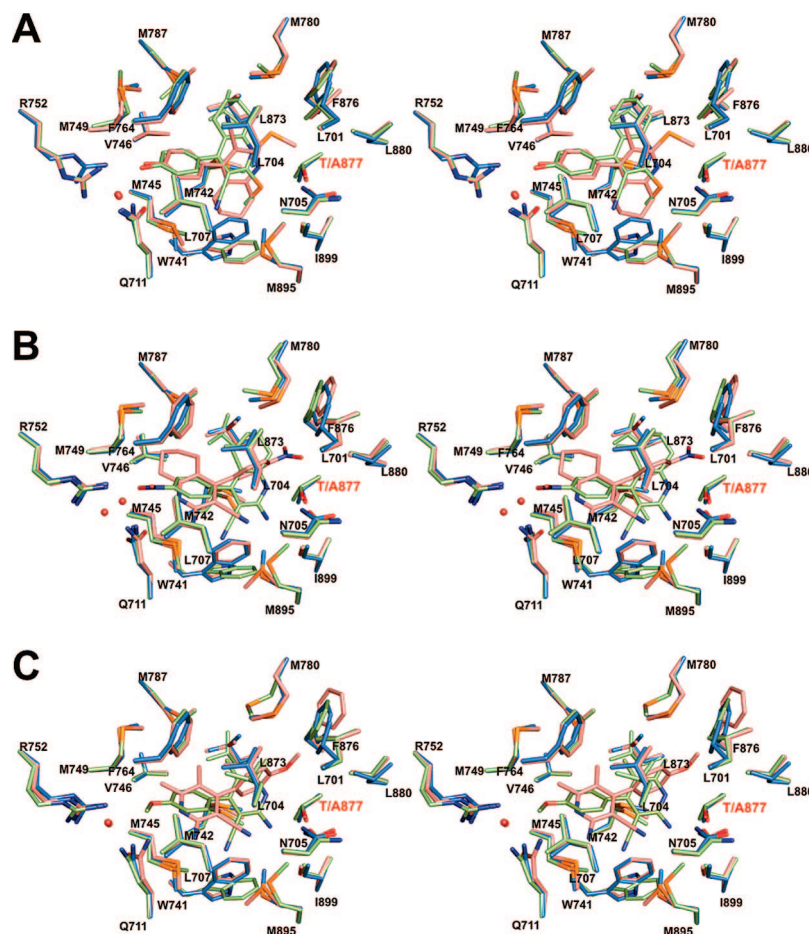


Figure 4. Stereo representations of the predicted interaction modes for compounds G1 (A), G2 (B), and G5 (C) in wild-type (green) and T877A mutated (pink) agonist structure of AR LBD. The T877A mutation frequently associated with prostate cancer is highlighted with a red label. The crystal structure of AR LBD (blue) is included as a reference for the side chain positions when interacting with the natural agonist DHT. (PDB id 1i37¹⁶) The ligand binding induced side chain movements needed to optimally fit G1, G2, and G5 to the binding sites of the two AR LBDs were predicted with the induced fit docking protocol of Schrödinger.²² Significant adjustments occur in W741 and M895 in the wild-type AR for all the compounds, while similar movements are only seen for G1 in the T877A mutant AR. These side chain adjustments may mechanistically be related to the origin of the AR antagonism demonstrated in experimental assays for these compounds in wild-type AR (G1, G2, and G5) and T877A mutant AR (G1).

type but not the mutant AR. Thus, one would not expect G5 to inhibit proliferation of LNCaP cells either. Finally, compound E5 turned out to be cytotoxic at 10 μ M concentration for this type of long-term treatment of LNCaP cells, and almost complete cell death incurred by day eight of the treatment. In contrast to this result, CV1 cells tolerated E5 at the same concentration in the reporter assay, which is likely the result of the shorter duration of treatment of cells.

Induced Fit Docking. Induced fit docking was performed to gain insight into the conformational changes that may occur in the binding site structure upon interaction with the reported antagonists, thereby offering some clues about the mechanism behind their antagonistic activity. Representative binding modes for compounds G1, G2, and G5 in both wild-type (green) and T877A mutant (pink) AR LBD structures, as well as the conformational changes induced to the receptor structures as predicted by our induced fit docking simulations are shown in Figure 4. In the wild-type LBP, all the compounds are predicted to bind with the phenyl ring substituent oriented toward the end of the pocket harboring the structural water molecule. Hydrogen bond interactions between the phenyl ring substituents and residues Q711, R752, and the water molecule are likely to occur. At the other end of the LBP, the aliphatic/alicyclic substituents of

the pyridine ring are predicted to occupy the upper part of the pocket, while the cyano and the amino/sulfide substituents fill the lower part of the pocket. While G1 forms mainly hydrophobic interactions with the binding site residues in this region, both the pyridine nitrogen and the amino substituent of G2 and G5 are capable of forming polar contacts because they are positioned within hydrogen bonding distance of T877. In the T877A mutant LBP, the binding mode for G1 is predicted to be flipped 180° along the plane of the phenyl ring, whereas G2 and G5 are predicted to be rotated 180° along the longest ligand axis compared to the wild-type structure. The hydrogen bond network between the hydroxyl group of G1 and the receptor seem to be conserved in the mutant binding site. G2 and G5 on the other hand appear to lose all the hydrogen bond interactions in their alternate binding mode in the mutant receptor.

The docking simulations suggest that binding of G1, G2, and G5 to the wild-type LBP entails reorientation of only a few residues, W741 and M895, in particular, when compared to their orientations in the crystal structure (blue) that was used as the starting structure for the induced fit dockings. These residues are also among the most flexible residues observed in experimentally determined structures of AR LBD bound to various ligands (Figure 5). In the mutant AR, a

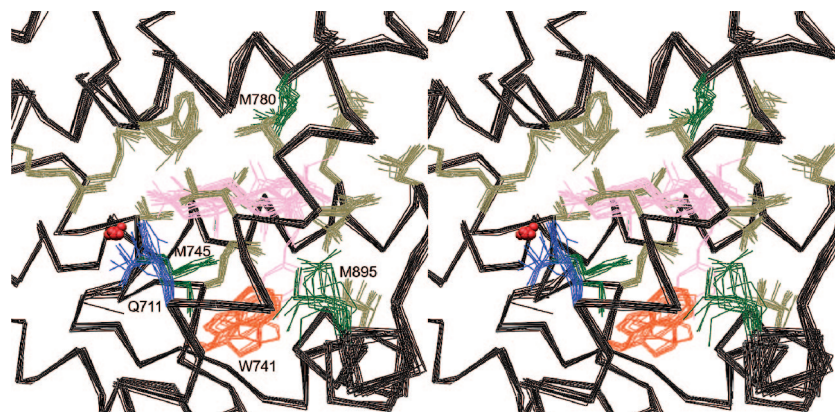


Figure 5. Superimposition of experimentally determined AR LBD agonist structures from the PDB (twenty ligand–receptor complex structures) show the side chains that can be induced into different conformation in the binding site by ligands. The protein structures are shown as black C α -trace and the bound ligands are shown as line representation in pink. The most flexible residues are orange (W741), green (M745/780/895), or blue (Q711), while the structurally more constrained residues are gray.

similar rearrangement is only observed when fitting G1 into the binding pocket.

On the basis of the induced fit docking results one can hypothesize that the antagonism observed for G1, G2, and G5 arises structurally from movement of residues W741 and M895 because there are no other major modifications predicted to take place according to these representative binding modes. The movement of these residues could in turn lead to more extensive structural changes required for antagonism.

DISCUSSION

Comparison to Antiandrogens Hydroxyflutamide and Bicalutamide. The nonsteroidal antiandrogen HF that is commonly used in the treatment of CaP undergoes an antagonist-to-agonist conversion in function during the progression of the disease. HF activity changes from antagonist to agonist in the LNCaP cells expressing mutant AR and the conversion into an agonist has been attributed to the T877A mutation residing in the ligand binding site of AR LBD.^{29,30} Structural evidence from the crystallographic studies supports this finding since AR LBD T877A mutant complexed with HF crystallizes in the agonist conformation.⁵ As a result, the T877A mutation overcomes the antagonist activity of HF in wild-type AR LBD and stimulates AR-mediated transcriptional activity instead.

Compound G5 shows behavior that is in part related to HF but also shows important differences. G5 inhibits transactivation of the wild-type AR but not of the T877A mutant AR. However, compared to HF, the compound G5 is not an agonist in transactivation experiments for the mutated AR (Figure 2B). G5 can be docked into the LBP of the T877A mutant without any receptor–ligand clashes or large side-chain movements in the binding site residues relative to the agonist bound AR LBP (Figure 4). However, the conversion of a threonine to alanine in the LBD reduces possibilities for G5 to make polar intermolecular interactions. Thus, one likely explanation for the lost antagonist activity and lack of agonist activity for the mutant AR could therefore be that G5 has a lower affinity for the mutant than the wild-type AR making it harder to compete in binding with R1881.

Bicalutamide is probably the most attractive nonsteroidal antiandrogen currently available for CaP treatment.^{1,31} As

with HF, AR mutations that cause resistance to bicalutamide antagonism are known,^{4,32} and they may occur during the progression of CaP. Bicalutamide retains, however, its antagonist behavior in T877A mutant AR^{5,30} and can be used as a second line of treatment after HF resistance following T877A mutation has occurred. According to our experimental assays a bicalutamide-like antagonist behavior was observed for the compounds G1 and G4 because they are able to act as antagonists in both wild-type and T877A mutant AR, although at a lower potency than bicalutamide.

Molecular Mechanisms of AR Antagonism. The experimentally determined structures of AR LBD in the PDB are invariably in the active, agonist conformation. Experimental knowledge of antagonist induced structural changes in AR LBD is lacking. Large-scale movements in NR LBDs have been documented for a few related receptors upon antagonist binding,^{33,34} for example, estrogen receptor (ER).^{35,36} In ER, antagonist ligands are able to interfere with the natural folding of the LBD by inhibiting positioning of helix 12 (H12) into its agonist conformation.^{33,35,36} Instead of taking the agonist position H12 swings onto the surface of AF2, which in agonist conformation of ER LBD serves as a binding surface for LxxLL motif containing coactivators^{36,37} and therefore inhibits coactivator binding. This can happen because an α -helical⁵⁴⁰ LLEML⁵⁴⁴ sequence in ER H12 is able to mimic the interactions between AF2 and coactivators. Interestingly, corresponding sequence in AR H12 is⁸⁹⁵ MAEII⁸⁹⁹. AR and ER LBDs are structurally highly similar, but there is no structural evidence that AR H12 could inhibit the AF2 surface in a similar fashion as in ER. Other mechanisms for AR antagonism have been proposed,^{30,38–41} but the molecular mechanism of AR antagonism remains unclear.

Superimposition of the active AR LBD structures deposited in the PDB illustrates the binding site residues that in crystal structures are shown to adapt and assume various positions when structurally diverse AR ligands are bound to the receptor (Figure 5). W741 and M895 are among the most flexible residues identified in the crystallographic experiments. They are especially important for induced accommodation of the large AR agonists into the LBP.^{5,8} M895, which is a H12 residue, has been the target of rational design of AR antagonists bearing a bulky extension connected to

steroid core with the objective of preventing correct positioning of H12 and consequently disrupting the functional AF2 surface.⁸ Both W741 and M895 have been shown to play a role in bicalutamide initiated antagonism too. For example, mutations W741L/W741C and M895T transform bicalutamide into an agonist that stimulates AR-mediated transcriptional activation.^{5,32} Valuable structural clues to the molecular mechanism for AR antagonism are additionally presented by cocrystal structures of antagonists with mutant AR LBD.^{4–7} These structures crystallized in the agonist conformation despite the bound antagonistic ligand. Altogether four antagonists, namely, the nonsteroidal bicalutamide,⁴ HF,⁵ and an isoindole-dione-based compound,⁷ and the steroidal cyproterone acetate,⁶ have been cocrystallized with mutant AR LBD structures. W741L and T877A variants of AR LBD have been used in the cocrystallization of bicalutamide and the other antagonists, respectively. Comparative analyses of the antagonist bound AR LBD structures to agonist bound wild-type structures of AR LBD suggest plausible explanations for why these compounds induce antagonist behavior in the wild-type AR. Taken together, the structural evidence suggests that a sterical overlap between M895 and bicalutamide has an important role in initiating the conformational changes upon bicalutamide-based antagonism.^{4,5} A clash between T877 and the other three antagonists is believed to be the source of the structural changes associated with their antagonism.^{5–7} These clashes are ultimately expected to induce displacement of H12 from its active position, thus disrupting the functional AF2 surface required for AR activity.

Taking into account these facts and apparent missing knowledge, we used induced-fit docking to elucidate effects that the discovered antagonists induce on the AR LBD. Because structural evidence does not indicate that AR LBD is antagonized by ligands through similar conformational changes as in, for example, ER,^{33,35,36} it seems unreasonable to build an antagonist model of AR LBD based on the known ER template. Rather, the identified AR antagonists were docked into an agonist structure (PDB id 1i37)¹⁶ using the induced fit docking methodology,²² which can account for both ligand and receptor flexibility. The receptor flexibility is addressed by side chain predictions and small movements in the protein backbone.

Antagonistic mechanism caused by ligands in AR could involve a large conformational change, as happens in the case of related ER. Large movements like repositioning of H12 cannot be reliably modeled with this methodology, and in general, movements and binding affinities are very difficult to predict using basic physical principles.^{42–44} Fortunately, only small adjustments in the AR binding site are needed to accommodate our compounds discovered in the VS, whose antagonistic mechanism was studied. Induced fit docking seems to be a sufficient tool to extend the modeling one step further to what can be achieved with GOLD by suggesting interaction points between binding ligand and protein, which in turn may induce more drastic effects in protein structure and function. However, it remains a challenge to fully simulate the changes induced by ligands to receptors with current computational methodologies.^{42–44}

Dockings were performed to both wild-type and T877A mutated LBD structures to mimic the AR cotransfected to CV1 cells and in cell proliferation assays and to try to

find possible structural explanation for the observed experimental results. Representative docking results to both wild-type and mutant structures are shown in Figure 4 for compounds G1, G2, and G5. When the compounds are docked into the wild-type AR structure, the most prominent side-chain adjustments take place in residues W741 and M895. The result is in agreement with residue movements in published crystallographic structures in PDB (Figure 5). The movement of the indole ring of W741 may indeed be needed to increase the binding site volume to fit the compounds and to enhance hydrogen bonding between the ligand and the receptor to, for example, T877. This movement also necessitates repositioning of the M895 side chain in the simulations. Because no overlap between the antagonists and T877 is detected, we hypothesize that the antagonism observed in the wild-type AR could result from structural changes initiated from repositioning of residues W741 and M895. On the other hand, when the compounds were fitted into the T877A mutant receptor, similar movements of both W741 and M895 side chains were only observed when docking compound G1. The additional space in the ligand binding pocket created by the T877A mutation seems to be enough to fit G2 and G5, but not the bulkier G1. According the docking simulations, the preferred binding modes of G2 and G5 in the mutant AR LBD are predicted to be flipped 180° compared to the wild-type structure. The change in the predicted binding modes proposes a lower binding affinity for these compounds toward mutant AR. Lower binding in turn would be reflected as reduced activity in the transactivation assay.

Overall, structural explanation from the docking studies correlates with the experimentally demonstrated compound activities. The results suggest that the antagonistic behavior of G1, G2, and G5 could be linked to movement of W741 and M895. The result is consistent with the experimental data provided by the mutation studies for bicalutamide.⁵

CONCLUSION

A panel of nonsteroidal AR binding compounds (E5, G1–G5) from a public chemical database were identified computationally and characterized in vitro for their functional activities. The in vitro results show the power of introduced VS procedure, which combines the 3D QSAR model and docking, in discovery of structurally new molecule classes for modulation of protein function, even though the measured potency of the discovered compounds was not as high as predicted by computations. The compounds are shown to bind to AR and are able to inhibit transactivation of human wild-type AR stimulated by the synthetic androgen R1881 in CV1 cells. Compounds E5, G2, G3, and G5 display somewhat more potent antagonist behavior than do G1 and G4. However, when a T877A mutation frequently present in CaP is introduced into the AR LBD, G1 and G4 emerge as the most powerful antagonists. The other compounds have reduced antagonistic activity compared to the wild-type receptor. The most obvious change took place for G5, which completely lost its' antagonistic potential. Compounds G1 and G4 were able to inhibit the proliferation of the prostate cancer LNCaP cells, expressing the T877A mutant AR. The

compound E5 also decreased the cell growth significantly, but the reduction was caused by toxic effects on the LNCaP cells. Interestingly, the cytotoxicity of E5 was not observed in transactivation experiments in CV1 cells. This may be because the CV1 cells were exposed to E5 for a shorter period of time than LNCaP cells used in the proliferation assay. The molecular mechanism by which AR antagonists, including those identified here, induce their inhibitory effect remains unknown, but residues W741 and M895 could be linked to the antagonistic ligand behavior. Further, derivatization of these novel nonsteroidal scaffolds could be the basis for new, more potent AR antagonists with inhibitory activity in both wild-type and T877A mutant AR.

ACKNOWLEDGMENT

This work was funded by the Academy of Finland and the Finnish Technology Agency (TEKES). Computational resources and program licenses were supplied by CSC—Scientific Computing Ltd.

REFERENCES AND NOTES

- Gao, W.; Kim, J.; Dalton, J. T. Pharmacokinetics and pharmacodynamics of nonsteroidal androgen receptor ligands. *Pharm. Res.* **2006**, *23*, 1641–1658.
- Buijsman, R. C.; Hermkens, P. H.; van Rijn, R. D.; Stock, H. T.; Teerhuis, N. M. Non-steroidal steroid receptor modulators. *Curr. Med. Chem.* **2005**, *12*, 1017–1075.
- Gottlieb, B.; Beitel, L. K.; Wu, J. H.; Trifiro, M. The androgen receptor gene mutations database (ARDB): 2004 update. *Hum. Mutat.* **2004**, *23*, 527–533.
- Bohl, C. E.; Gao, W.; Miller, D. D.; Bell, C. E.; Dalton, J. T. Structural basis for antagonism and resistance of bicalutamide in prostate cancer. *Proc. Natl. Acad. Sci. U.S.A.* **2005**, *102*, 6201–6206.
- Bohl, C. E.; Miller, D. D.; Chen, J.; Bell, C. E.; Dalton, J. T. Structural basis for accommodation of nonsteroidal ligands in the androgen receptor. *J. Biol. Chem.* **2005**, *280*, 37747–37754.
- Bohl, C. E.; Wu, Z.; Miller, D. D.; Bell, C. E.; Dalton, J. T. Crystal structure of the T877A human androgen receptor ligand-binding domain complexed to cyproterone acetate provides insight for ligand-induced conformational changes and structure-based drug design. *J. Biol. Chem.* **2007**, *282*, 13648–13655.
- Salvati, M. E.; Balog, A.; Shan, W.; Wei, D. D.; Pickering, D.; Attar, R. M.; Geng, J.; Rizzo, C. A.; Gottardis, M. M.; Weinmann, R.; Krystek, S. R.; Sack, J.; An, Y.; Kish, K. Structure based approach to the design of bicyclic-1H-isoindole-1,3(2H)-dione based androgen receptor antagonists. *Bioorg. Med. Chem. Lett.* **2005**, *15*, 271–276.
- Cantin, L.; Faucher, F.; Couture, J. F.; de Jesus-Tran, K. P.; Legrand, P.; Ciobanu, L. C.; Frechette, Y.; Labrecque, R.; Singh, S. M.; Labrie, F.; Breton, R. Structural characterization of the human androgen receptor ligand-binding domain complexed with EM5744, a rationally designed steroidal ligand bearing a bulky chain directed toward helix 12. *J. Biol. Chem.* **2007**, *282*, 30910–30919.
- Berman, H. M.; Westbrook, J.; Feng, Z.; Gilliland, G.; Bhat, T. N.; Weissig, H.; Shindyalov, I. N.; Bourne, P. E. The Protein Data Bank. *Nucleic Acid Res.* **2000**, *28*, 235–242.
- Söderholm, A. A.; Lehtovuori, P. T.; Nyrönen, T. H. Three-dimensional structure-activity relationships of nonsteroidal ligands in complex with androgen receptor ligand-binding domain. *J. Med. Chem.* **2005**, *48*, 917–925.
- Cramer III, R. D.; Patterson, D. E.; Bunce, J. D. Comparative molecular field analysis (CoMFA) 1. Effect of shape on binding of steroids to carrier proteins. *J. Am. Chem. Soc.* **1988**, *110*, 5959–5967.
- Klebe, G.; Abraham, U.; Mietzner, T. Molecular similarity indices in a comparative analysis (CoMSIA) of drug molecules to correlate and predict their biological activity. *J. Med. Chem.* **1994**, *37*, 4130–4146.
- Jones, G.; Willett, P.; Glen, R. C.; Leach, A. R.; Taylor, R. Development and validation of a genetic algorithm for flexible docking. *J. Mol. Biol.* **1997**, *267*, 727–748.
- Moehren, U.; Dressel, U.; Reeb, C. A.; Vaisanen, S.; Dunlop, T. W.; Carlberg, C.; Baniahmad, A. The highly conserved region of the co-repressor Sin3A functionally interacts with the co-repressor Alien. *Nucleic Acids Res.* **2004**, *32*, 2995–3004.
- Protopopov, A. I.; Li, J.; Winberg, G.; Gizatullin, R. Z.; Kashuba, V. I.; Klein, G.; Zabarovsky, E. R. Human cell lines engineered for tetracycline-regulated expression of tumor suppressor candidate genes from a frequently affected chromosomal region, 3p21. *J. Gene Med.* **2002**, *4*, 397–406.
- Sack, J. S.; Kish, K. F.; Wang, C.; Attar, R. M.; Kiefer, S. E.; An, Y.; Wu, G. Y.; Scheffler, J. E.; Salvati, M. E.; Krystek, S. R., Jr.; Weinmann, R.; Einspahr, H. M. Crystallographic structures of the ligand-binding domains of the androgen receptor and its T877A mutant complexed with the natural agonist dihydrotestosterone. *Proc. Natl. Acad. Sci. U.S.A.* **2001**, *98*, 4904–4909.
- Maestro, version 8.0; Schrödinger, LLC: New York, 2007.
- Prime, version 1.6; Schrödinger, LLC: New York, 2007.
- Sadowski, J.; Gasteiger, J. From atoms and bonds to three-dimensional atomic coordinates: model builders. *Chem. Rev.* **1993**, *93*, 2567–2581.
- Sadowski, J.; Gasteiger, J.; Klebe, G. Comparison of automatic three-dimensional model builders using 639 x-ray structures. *J. Chem. Inf. Comput. Sci.* **1994**, *34*, 1000–1008.
- Impact, version 4.5; Schrödinger, LLC: New York, 2005.
- Schrödinger Suite 2007 Induced Fit Docking protocol. *Glide*, version 4.5; Schrödinger, LLC: New York, 2005; *Prime*, version 1.6; Schrödinger, LLC: New York, 2005.
- Sherman, W.; Day, T.; Jacobson, M. P.; Friesner, R. A.; Farid, R. Novel procedure for modeling ligand/receptor induced fit effects. *J. Med. Chem.* **2006**, *49*, 534–553.
- Wang, R.; Lu, Y.; Fang, X.; Wang, S. An extensive test of 14 scoring functions using the PDBbind refined set of 800 protein-ligand complexes. *J. Chem. Inf. Comput. Sci.* **2004**, *44*, 2114–2125.
- Wang, R.; Lu, Y.; Wang, S. Comparative evaluation of 11 scoring functions for molecular docking. *J. Med. Chem.* **2003**, *46*, 2287–2303.
- Warren, G. L.; Andrews, C. W.; Capelli, A. M.; Clarke, B.; LaLonde, J.; Lambert, M. H.; Lindvall, M.; Nevins, N.; Semus, S. F.; Senger, S.; Tedesco, G.; Wall, I. D.; Woolven, J. M.; Peishoff, C. E.; Head, M. S. A critical assessment of docking programs and scoring functions. *J. Med. Chem.* **2006**, *49*, 5912–5931.
- Moehren, U.; Papaioannou, M.; Reeb, C. A.; Hong, W.; Baniahmad, A. Alien interacts with the human androgen receptor and inhibits prostate cancer cell growth. *Mol. Endocrinol.* **2007**, *21*, 1039–1048.
- Taplin, M. E.; Bubley, G. J.; Ko, Y. J.; Small, E. J.; Upton, M.; Rajeshkumar, B.; Balk, S. P. Selection for androgen receptor mutations in prostate cancers treated with androgen antagonist. *Cancer Res.* **1999**, *59*, 2511–2515.
- Veldscholte, J.; Ris-Stalpers, C.; Kuiper, G. G.; Jenster, G.; Berrevoets, C.; Claassen, E.; van Rooij, H. C.; Trapman, J.; Brinkmann, A. O.; Mulder, E. A mutation in the ligand binding domain of the androgen receptor of human LNCaP cells affects steroid binding characteristics and response to anti-androgens. *Biochem. Biophys. Res. Commun.* **1990**, *173*, 534–540.
- Veldscholte, J.; Berrevoets, C. A.; Brinkmann, A. O.; Grootegeed, J. A.; Mulder, E. Anti-androgens and the mutated androgen receptor of LNCaP cells: differential effects on binding affinity, heat-shock protein interaction, and transcription activation. *Biochemistry* **1992**, *31*, 2393–2399.
- Gao, W.; Bohl, C. E.; Dalton, J. T. Chemistry and structural biology of androgen receptor. *Chem. Rev.* **2005**, *105*, 3352–3370.
- Hara, T.; Miyazaki, J.; Araki, H.; Yamaoka, M.; Kanzaki, N.; Kusaka, M.; Miyamoto, M. Novel mutations of androgen receptor: a possible mechanism of bicalutamide withdrawal syndrome. *Cancer Res.* **2003**, *63*, 149–153.
- Bourguet, W.; Germain, P.; Gronemeyer, H. Nuclear receptor ligand-binding domains: three-dimensional structures, molecular interactions and pharmacological implications. *Trends Pharmacol. Sci.* **2000**, *21*, 381–388.
- Nagy, L.; Schwabe, J. W. Mechanism of the nuclear receptor molecular switch. *Trends Biochem. Sci.* **2004**, *29*, 317–324.
- Brzozowski, A. M.; Pike, A. C.; Dauter, Z.; Hubbard, R. E.; Bonn, T.; Engstrom, O.; Ohman, L.; Greene, G. L.; Gustafsson, J. A.; Carlquist, M. Molecular basis of agonism and antagonism in the oestrogen receptor. *Nature* **1997**, *389*, 753–758.
- Shiau, A. K.; Barstad, D.; Loria, P. M.; Cheng, L.; Kushner, P. J.; Agard, D. A.; Greene, G. L. The structural basis of estrogen receptor/coactivator recognition and the antagonism of this interaction by tamoxifen. *Cell* **1998**, *95*, 927–937.
- Heery, D. M.; Kalkhoven, E.; Hoare, S.; Parker, M. G. A signature motif in transcriptional co-activators mediates binding to nuclear receptors. *Nature* **1997**, *387*, 733–736.
- Masiello, D.; Cheng, S.; Bubley, G. J.; Lu, M. L.; Balk, S. P. Bicalutamide functions as an androgen receptor antagonist by assembly of a transcriptionally inactive receptor. *J. Biol. Chem.* **2002**, *277*, 26321–26326.

- (39) Dotzlaw, H.; Moehren, U.; Mink, S.; Cato, A. C.; Iniguez Lluhi, J. A.; Baniahmad, A. The amino terminus of the human AR is target for corepressor action and antihormone agonism. *Mol. Endocrinol.* **2002**, *16*, 661–673.
- (40) Farla, P.; Hersmus, R.; Trapman, J.; Houtsmuller, A. B. Antiandrogens prevent stable DNA-binding of the androgen receptor. *J. Cell. Sci.* **2005**, *118*, 4187–4198.
- (41) Hodgson, M. C.; Astapova, I.; Cheng, S.; Lee, L. J.; Verhoeven, M. C.; Choi, E.; Balk, S. P.; Hollenberg, A. N. The androgen receptor recruits nuclear receptor CoRepressor (N-CoR) in the presence of mifepristone via its N and C termini revealing a novel molecular mechanism for androgen receptor antagonists. *J. Biol. Chem.* **2005**, *280*, 6511–6519.
- (42) Bren, U.; Martinek, V.; Florian, J. Free energy simulations of uncatalyzed DNA replication fidelity: structure and stability of T.G and dTTP.G terminal DNA mismatches flanked by a single dangling nucleotide. *J. Phys. Chem. B.* **2006**, *110*, 10557–10566.
- (43) Florian, J.; Goodman, M. F.; Warshel, A. Computer simulations of protein functions: searching for the molecular origin of the replication fidelity of DNA polymerases. *Proc. Natl. Acad. Sci. U.S.A.* **2005**, *102*, 6819–6824.
- (44) Matkar, R. A.; Kyu, T. Role of crystal-amorphous interaction in phase equilibria of crystal-amorphous polymer blends. *J. Phys. Chem. B.* **2006**, *110*, 12728–12732.

CI800149W